

Fluid production behavior of water-saturated hydrate-bearing sediments below the quadruple point of CH₄+H₂O

Qing-Cui Wan^{1,2,3}, Zhenyuan Yin^{3*}, Hu Si^{1,2*}, Praveen Linga^{3*}

¹ State Key Laboratory of Coal Mine Disaster Dynamics and Control, Chongqing University, Chongqing 400044, China

² School of Resources and Safety Engineering, Chongqing University, Chongqing 400044, China

³ National University of Singapore, Department of Chemical and Biomolecular Engineering, Singapore 117582

* (Corresponding Author)

ABSTRACT

In this study, we focus on the fluid production behavior of water-saturated hydrate-bearing sediments with hydrate saturation around 40% induced by depressurization below the quadruple point of CH₄+H₂O, which was rarely reported in the open literature. We conducted a series of experiments with ultra-deep depressurization of 1.0 MPa, 1.5 MPa and 2.1 MPa to investigate the gas and water production profiles. Ultra-fast gas production was observed with staged water production profile. Ice formation and secondary hydrate formation was likely based on the temperature measurement. However, the concurrence of ice formation did not promote the gas production significantly due to the large driving force that has already been induced by the ultra-deep depressurization. Various hydrate saturations between 20-60 vol% and pressure drawdown rates were also employed to further optimize the production condition below the quadruple point in the full paper.

Keywords: Natural Gas Hydrate; Ultra-deep Depressurization; Quadruple Point; Water-Saturated Hydrate-bearing Sediments; Fluid production; Heat Transfer

1. INTRODUCTION

Natural gas hydrate (NGH), a type of crystalline solid compound composed of natural gas which is trapped in crystal lattice cages formed by water molecules, are considered as a promising alternative energy for the future [1]. Naturally occurring gas hydrate are widely distributed in deep ocean sediments and permafrost locations. The global potential volume of methane trapped in NGHs is estimated to be 3000 trillion cubic

meters [2]. Driven by the abundant reserves, various gas production technologies have been proposed to recover methane from hydrate bearing sediments: including depressurization [3], thermal stimulation [4], CO₂ replacement [5], and thermodynamic inhibitor injection [6]. From the perspective of technical and economic feasibility and environmental aspects, depressurization has been regarded as the most energy-efficient method [7] in recovering gas from hydrate-bearing sediments because of no additional energy consumption during the production course. This method has been conducted in several field tests such as China Shenhu area [8], Japan Nankai Trough [9] and Canada Mallik test site [10].

However, a large body of hydrate dissociation are conducted above the quadruple point of CH₄ + H₂O system ($P = 2.1$ MPa). Few studies are focused on the fluid production below the quadruple point. And debates exist on the gas hydrate dissociation induced by depressurization below the quadruple point.

When the system pressure is dropped below the quadruple point, there are four phase coexisting in the system: gas, water, CH₄-hydrate and ice. Moridis et al. [11] reported that ice clogging slowed down gas production rate. However, Konno et al. [12] conducted gas production in a large reservoir simulator - a high pressure giant Unit (1710.0L) by depressurization. They found that the hydrate could not be totally dissociated by depressurization above the quadruple point in such large-scale reactor. But when they decreased the system pressure below the quadruple point with $P < 2.1$ MPa, the gas production was accelerated. They demonstrated that the intentional ice formation can potentially promote the gas recovery.

Wang et al. [13] investigated the methane hydrate dissociation behavior below the quadruple point at 2.1-2.5MPa. The initial saturation of hydrate in their work was about 30% with a predominately high gas saturation, $S_G = 50\%$. They concluded that the dissociation rate of the hydrate were greatly boosted because of the latent heat released by ice formation. Sun et al. [14] conducted the methane hydrate dissociation experiments below the freezing point at 1.8-2.2 MPa with $S_H = \sim 27\%$ and $S_G = \sim 44\%$. They pointed out that the supercooled water below the freezing point could slow down the gas production rate. But the ice formation would promote gas production.

In brief, the methane hydrate dissociation below the quadruple point is a controversial topic. Furthermore, previous studies usually focused on the pressure in the range of 1.8-2.5 MPa in sediments with high gas saturations. The effect of deep depressurization on hydrate dissociation below freezing point in aqueous-rich hydrate-bearing sediments is still not clear, which is of great significance for the exploitation of water-saturated marine gas hydrate deposits. Therefore, this study aims to investigate the gas recovery behavior under deep depressurization ($P = 1.0$ MPa-2.1 MPa) below the quadruple point in aqueous-rich hydrate-bearing sediments.

2. EXPERIMENTAL SECIOTN

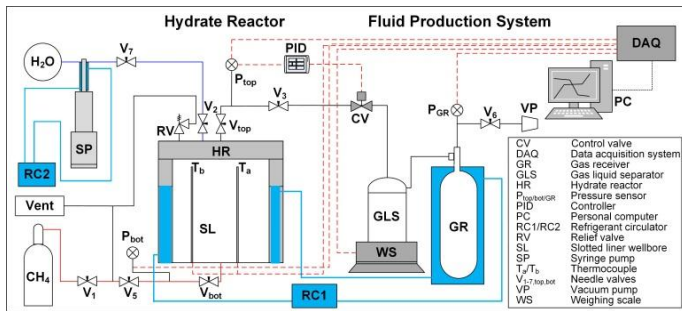


Fig. 1 A schematic of the experimental setup for hydrate-bearing sediments formation and dissociation

Fig. 1 shows the schematic drawing of the experimental setup used for methane hydrate formation and dissociation. It is a cylindrical pressure vessel with the effective inner volume of 980mL ($D = 102$ mm, $H = 120$ mm). To monitor the temperature change in the reactor, two multipoint thermocouples were installed at various positions ($r_a = 25$ mm, $r_b = 38$ mm) from the reactor center. The detailed setup can be found in our previous study [15].

For the formation step, the unconsolidated fine sands were filled up into the vessel tightly with a

porosity of 43%. Subsequently, a designed amount of pure methane gas and deionized water were injected into the reactor for methane hydrate formation. The hydrate generation was triggered by the cooling of vessel to 274.2K through the circulating water surrounding the reactor wall. When the final pressure went stable ($\Delta P \leq 10$ kPa/hr), the aqueous-rich hydrate sample was obtained. Then, the system will be increased from 274.2 K to 281.2 K step by step to mimic the temperature condition of about 130 meters below seafloor based on the geothermal gradient of 3.0 K per 100m.

For the dissociation step, the valve (V_{top}) was opened to drop the pressure from around 8.5 MPa to 6.0 MPa. Then the depressurization and the fluid production process began from the same $P = 6.0$ MPa for fair comparison. In this work, the production pressure was controlled by the control valve coupled with a PID controller below the quadruple point at $P = 2.1$ MPa (R1), 1.5 MPa (R2), 1.0 MPa (R3), respectively. This aims to investigate the effect of the degree of deep pressure drawdown on the hydrate dissociation. Additionally, experiments were also conducted to elucidate the controlling factor for fluid production from water-saturated hydrate-bearing sediments below the quadruple point, specifically on (a) pressure drawdown rate; and (b) the initial hydrate phase saturation and will be presented in the full paper.

3. RESULTS AND DISCUSSIONS

3.1 CUMULATIVE FLUID PRODUCTION PROFILE

Table 1. summarizes the conditions of the three sets of methane hydrate formation. Pore-volume balance method considering all three phases [16] was used to estimate the overall phase saturation in the reactor. It could be observed that the prepared methane hydrate bearing samples have similar phase saturations, indicating the reliability of the synthesizing method we used. Furthermore, the obtained high hydrate saturation ($S_H > 40\%$) with low gas saturation $S_G = \sim 2\%$ can well represent the naturally occurring hydrate-bearing sediments, which is meaningful for future field applications.

Table 1. Summary of the experimental conditions and saturations of three phases at the end of the hydrate formation process

| Run | Mass of Sand (g) | P_G (kPa) | V_w (g) | S_H | S_G | S_A |
|-----|------------------|-------------|-----------|--------|-------|--------|
| R1 | 1480.43 | 6.6 | 417.61 | 42.62% | 2.02% | 55.36% |
| R2 | 1480.44 | 6.7 | 415.78 | 42.99% | 2.34% | 54.66% |
| R3 | 1480.44 | 6.7 | 416.99 | 42.96% | 2.09% | 54.95% |

Table 2. Summary of the experimental conditions and the results of fluid production and recovery in the dissociation process

| Run | P_{end} (MPa) | P_{GR} (KPa) | $n_{G,F}$ (mol) | R_G (%) | $n_{W,F}$ (mol) | R_W (%) | WGR (mol/mol) |
|-----|-----------------|----------------|-----------------|-----------|-----------------|-----------|---------------|
| R1 | 1.0 | 607.56 | 1.398 | 91.09 | 9.64 | 41.55 | 6.89 |
| R2 | 1.5 | 587.58 | 1.385 | 88.94 | 8.21 | 35.57 | 5.93 |
| R3 | 2.1 | 582.14 | 1.35 | 87.07 | 6.46 | 27.89 | 4.78 |

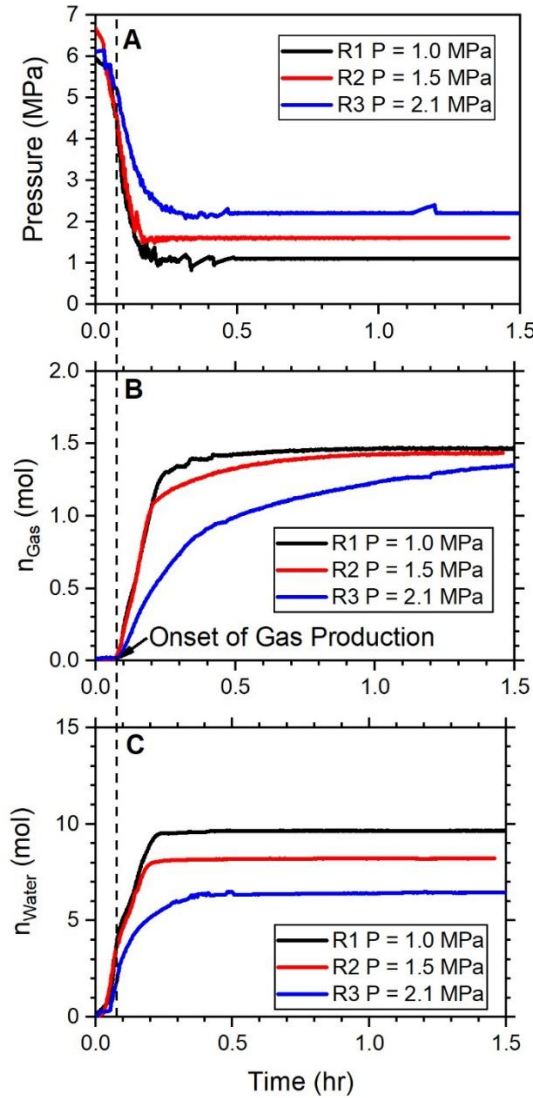


Fig. 2. Evolution of (A) pressure, (B) cumulative production of gas and (C) cumulative production of water during the dissociation process below the quadruple point

Fig. 2A shows the evolution of the system pressure over time. The entire dissociation process lasted for around 1.5 hr, when the cumulative production of both gas and water plateaued. Pressure drawdown rate was similar for Case R1 and R2 and was slightly slower in Case R3, where BHP drops from initial $P = 6.0$ MPa to its final level within 0.3 hr. BHP was maintained constant at 1.0 MPa in Case R1, 1.5 MPa in Case R2 and 2.1 MPa in Case R3 throughout the rest of the dissociation duration.

Fig. 2B shows the evolution of cumulative gas production over time. It is evident that decreasing the pressure from 2.1 MPa to 1.0 MPa increases the final gas recovery from 87.1% to 91.1%. In addition, it was observed that the rate of gas production is closely related to the rate of pressure decrease shown in Fig. 2A. Gas production reached its final level within 0.5 hr for Case R1 and R2 with P below the quadruple point, while gas was continuously produced over the period of 1.5 hr with $P = 2.1$ MPa. Such gas production profile suggests that depressurization below the quadruple point promotes gas production. In addition, onset of gas production is not immediate upon depressurization, but only start at $t = 0.08$ hr when P drops below 4.8 MPa. This is attributed to the extreme low initial gas saturation in the deposit (about 2 vol% in Table 1). The majority of CH_4 are restricted in hydrates and can only be released when the system P drops below the equilibrium pressure, $P_{eq} = 5.7$ MPa at 281.2 K. Such gas production behaviors is typical of water-saturated hydrate-bearing sediments [17] and differ from those in gas-saturated condition, where gas production starts immediately upon dissociation [7, 17].

Comparatively, water can be produced immediately upon depressurization as shown in Fig. 2C. This can be attributed to the high initial water saturation in the reactor around 55 vol%. The free water can be produced readily upon pressure drawdown. In addition, based on the final cumulative volume of water produced, it can be concluded that decreasing the pressure from 2.1 to 1.0 MPa increases the final water recovery ratio by 1.5 times from 27.9% to 41.6%. No significant benefit of trapping the free water for ice formation was observed by dropping pressure below the quadruple point. It is also interesting to note that water production was not continuous thoroughly the dissociation and only lasted for the 0.2 hr for Case R1 and R2, and 0.5 hr for Case R3. No significant amount of water was produced during the constant pressure stage. The staged water production profile could have potential implication in addressing field-scale production, where excess water production is likely to happen at the initial stage of depressurization. Energy efficiency ratio and the water-gas ratio will be further analyzed in the full paper to further evaluation the optimal condition for gas production and recovery.

3.2 TEMPERATURE RESPONSE AND EVOLUTION

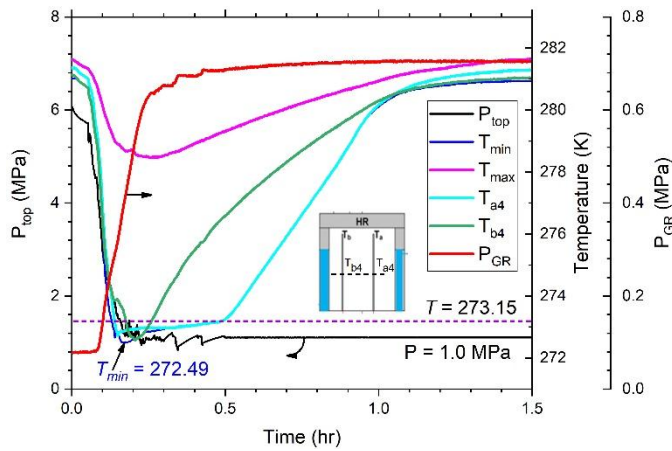


Fig. 3. Evolution of pressure (P_{top} , P_{GR}) and temperature (T_{min} , T_{min} , T_{a4} and T_{b4}) over time in Case R1 with $P = 1.0$ MPa.

Fig. 3 shows the evolution of temperature (minimum temperature registered in all twelve thermal couple (T_{min}), maximum temperature registered in all twelve thermal couples (T_{max}), temperature at specific positions T_{a4} and T_{b4} see the small panel in Fig. 3) over time with the presentation of pressure at reactor outlet top position (P_{top}) and the gas reservoir (P_{GR}). Initial sharp decrease of T was observed upon depressurization. The lowest T reached is 272.49 K, around 0.66 K below the quadruple point of H_2O . A small peak was observed at $t = 0.18$ hr when T_{min} reached its lowest value suggesting ice formation due to the exothermic reaction. However, no significant increase in P_{GR} was observed mainly because the hydrate dissociation is already fast under low BHP = 1.0 MPa. The additional formation of ice does not contribute more to the gas production.

Examining T_{min} and T_{max} in Fig. 3 shows that there is a maximum temperature difference around 6.5 K at $t = 0.2$ hr. This clearly indicates that the distribution of T is non-uniform across the entire reactor. This can be attributed to the heterogeneous hydrate distribution during formation as analyzed in a detailed numerical study of MH formation in the same reactor [18].

The heat transfer direction can be informed from the evolution of T_{a4} and T_{b4} in Fig. 3. Both positions have similar vertical position but different radial length from the reactor center. T_{b4} (represented by the green curve) shows a higher T than T_{a4} (represented by the cyan curve) during the entire depressurization process until $t = 1.0$ hr. Thus, the direction of heat transfer is from reactor outer boundary to the inner center during this period. In addition, a longer period was observed at T_{a4} position with T around 273.15 K. We could infer that the hydrate saturation could be higher at T_{a4} position with more heat required for hydrate dissociation. The spatial

distribution of T over time in different experimental cases will be further analyzed in the full paper.

CONCLUSION

Ultra-deep depressurization could be one technical feasible and economic viable optional in increasing the rate of gas production and final gas recovery ratio. However, the low temperature induced by the fast hydrate dissociation rate could result in ice or secondary hydrate formation. In laboratory, heat transfer from ambient surrounding could mitigate the low temperature issue. However, in field production tests, such low T below 273.15 K in ultra-deep depressurization test could result in flow assurance issues and the adoption should be employed and evaluated carefully. Hydrate phase saturation and pressure drawdown rate should be selected carefully to mitigate the low T issue. These contributing factors will be further elucidated in the full paper of this abstract.

ACKNOWLEDGEMENT

The financial support from National University of Singapore (NUS) is greatly appreciated (R-279-000-542-114). Qingcui Wan acknowledges the support from the state scholarship fund from China Scholarship Council (No. 201906050104).

REFERENCE

- [1] Sloan ED, Koh C.A.,. Clathrate Hydrates of Natural Gases, 3rd Edition., CRC Press, Boca Raton, FL. 2008.
- [2] Boswell R, Collett TS. Current perspectives on gas hydrate resources. *Energy Environ Sci.* 2011;4:1206-15.
- [3] Yin ZY, Moridis G, Chong ZR, Tan HK, Linga P. Numerical analysis of experimental studies of methane hydrate dissociation induced by depressurization in a sandy porous medium. *Appl Energy.* 2018;230:444-59.
- [4] Li B, Liu SD, Liang YP, Liu H. The use of electrical heating for the enhancement of gas recovery from methane hydrate in porous media. *Appl Energy.* 2018;227:694-702.
- [5] Xu CG, Cai J, Yu YS, Yan KF, Li XS. Effect of pressure on methane recovery from natural gas hydrates by methane-carbon dioxide replacement. *Appl Energy.* 2018;217:527-36.
- [6] Yuan Q, Sun CY, Wang XH, Zeng XY, Yang X, Liu B, et al. Experimental study of gas production from hydrate dissociation with continuous injection mode using a three-dimensional quiescent reactor. *Fuel.* 2013;106:417-24.

- [7] Yang MJ, Fu Z, Jiang LL, Song YC. Gas recovery from depressurized methane hydrate deposits with different water saturations. *Appl Energy*. 2017;187:180-8.
- [8] Li JF, Ye JL, Qin XW, Qiu HJ, Wu NY, Lu HL, et al. The first offshore natural gas hydrate production test in South China Sea. *China Geol*. 2018;1:5-16.
- [9] Yamamoto K, Wang XX, Tamaki M, Suzuki K. The second offshore production of methane hydrate in the Nankai Trough and gas production behavior from a heterogeneous methane hydrate reservoir. *RSC Adv*. 2019;9:25987-6013.
- [10] Moridis GJ, Collett TS, Dallimore SR, Satoh T, Hancock S, Weatherill B. Numerical studies of gas production from several CH₄ hydrate zones at the Mallik site, Mackenzie Delta, Canada. *Journal of Petroleum Science and Engineering*. 2004;43:219-38.
- [11] Moridis GJ, Collett TS, Boswell R, Kurihara M, Reagan MT, Koh C, et al. Toward Production From Gas Hydrates: Current Status, Assessment of Resources, and Simulation-Based Evaluation of Technology and Potential. *SPE Reserv Eval Eng*. 2009;12:745-71.
- [12] Konno Y, Jin Y, Shinjou K, Nagao J. Experimental evaluation of the gas recovery factor of methane hydrate in sandy sediment. *RSC Adv*. 2014;4:51666-75.
- [13] Wang Y, Feng J-C, Li X-S, Zhang Y, Li G. Large scale experimental evaluation to methane hydrate dissociation below quadruple point in sandy sediment. *Appl Energy*. 2016;162:372-81.
- [14] Sun RH, Fan Z, Yang MJ, Pang WX, Li YP, Song YC. Experimental investigation into the dissociation of methane hydrate near ice-freezing point induced by depressurization and the concomitant metastable phases. *J Nat Gas Sci Eng*. 2019;65:125-34.
- [15] Chong ZR, Yin ZY, Tan JHC, Linga P. Experimental investigations on energy recovery from water-saturated hydrate bearing sediments via depressurization approach. *Appl Energy*. 2017;204:1513-25.
- [16] Yin Z, Moridis G, Chong ZR, Linga P. Effectiveness of multi-stage cooling processes in improving the CH₄-hydrate saturation uniformity in sandy laboratory samples. *Appl Energy*. 2019;250:729-47.
- [17] Gao Q, Yin Z, Zhao J, Yang D, Linga P. Tuning the fluid production behaviour of hydrate-bearing sediments by multi-stage depressurization. *Chemical Engineering Journal*. 2021;406:127174.
- [18] Yin Z, Moridis G, Tan HK, Linga P. Numerical analysis of experimental studies of methane hydrate formation in a sandy porous medium. *Appl Energy*. 2018;220:681-704.